Platinum Orthometalated Liquid Crystals Compared with Their Palladium Analogues. First Optical Storage Effect in an Organometallic Liquid Crystal

Julio Buey,[†,‡] Laura Díez,[†] Pablo Espinet,*[,†] Heinz-S. Kitzerow,*[,†] and Jesús A. Miguel[†]

Química Inorgánica, Facultad de Ciencias, Universidad de Valladolid, E-47005 Valladolid, Spain, and Iwan-N.-Stranski- Institut, Technische Universität Berlin, Sekr. ER 11, Strasse des 17 Juni 135, D-10623 Berlin, Germany

Received March 26, 1996. Revised Manuscript Received June 11, 1996[⊗]

Di-μ-chlorobis(η^3-2-methylallylplatinum) reacts with imines HL_n = *p*-$C_nH_{2n+1}O-C_6H_4-CH{=}N-C_6H_4-OC_nH_{2n+1}$-*p* ($n$ = 6, **1a**; n = 2, **1b**) to yield the C,N-cyclometalated platinum(II) compounds $[Pt_2(\mu\text{-}Cl)_2(L_n)_2]$ (**2a**, **2b**). From **2**, other types of dinuclear complexes $[Pt_2(\mu\text{-}X)_2(L_n)_2]$ with X = OAc, (*R*)-2-chloropropionato, SC_nH_{2n+1}), mixed bridged complexes $[Pt_2(\mu\text{-}X)(\mu\text{-}Y)(L_n)_2]$ (X = Cl, OAc, (*R*)-2-chloropropionato; Y = SC_nH_{2n+1}), and mononuclear complexes [Pt(acac)(L_n)] have been prepared, and their mesogenic properties are compared with those of their palladium analogues reported previously. The Pt compounds exhibit higher temperature transitions, unless a different composition hides this effect when the material is a mixture of isomers. One of the compounds, *cis*-$[Pt_2(\mu\text{-}X)(\mu\text{-}Y)(L_n)_2]$ (X = (*R*)-2-chloropropionato; Y = $SC_{16}H_{33}$), forms a glasslike state on cooling from the cholesteric phase and shows absorption of light in the visible wavelength range. As a consequence, it is suitable for optooptical storage effects, which have been realized on the complex without the addition of dye.

Introduction

A large and prominent family of metallomesogens (metal-containing compounds displaying liquid-crystalline behavior)[1] is that of organometallic complexes derived from orthopalladated imines and azines,[2] as well as azobenzene, azoxybenzene, and phenylpyrimidines.[3]

This class of mesogens is represented by palladium derivatives mainly, due to the ease of the orthopaladation reaction. Very recently orthometalated mesogens of Hg and Mn have been described.[4,5]

Easy orthoplatination became accessible recently using $[Pt_2(\mu\text{-}Cl)_2(\eta^3\text{-}C_4H_7)_2]$ as starting material.[6] Following our communication on the synthesis of calamitic orthoplatinated mesogens,[7] Praefcke et al. have described several discotic di- or tetraplatinum organyls giving rise to columnar phases.[8,9] They have found that the change of the metal (Pt or Pd) has a minor influence in the thermotropic or the lyotropic properties of these large disk-shaped di- or tetraplatinum organyls.[9]

In this paper we report monomeric and dimeric calamitic orthoplatinated complexes. Comparing their properties with those of their Pd analogues, we find a significant influence of the nature of the metal. One of the compounds produces a glasslike cholesteric phase which can be used for optical storage.

Experimental Section

Literature methods were used to prepare di-μ-chlorobis(η^3-2-methylallylplatinum),[10] potassium (*R*)-2-chloropropionate,[11] $AgSC_nH_{2n+1}$,[12] and thallium acetylacetonate;[13] the imines HL_n were synthesized by acetic acid catalyzed condensation of the corresponding aldehyde and amine in absolute ethanol.[14] C, H, N analyses were carried out on a Perkin-Elmer 2400

[†] Universidad de Valladolid.
[‡] Technische Universität Berlin.
[⊗] Abstract published in *Advance ACS Abstracts,* August 1, 1996.

(1) For reviews see: (a) Giroud-Godquin, A. M.; Maitlis, P. M. *Angew. Chem., Int. Ed. Engl.* **1991**, *30*, 375. (b) Espinet, P.; Esteruelas, M. A.; Oro, L. A.; Serrano, J. L.; Sola, E. *Coord. Chem. Rev.* **1992**, *117*, 215. (c) Bruce, D. W. *Inorganic Materials*; Bruce, D. W.; O'Hare, D., Eds.; John Wiley & Sons: Chichester, Great Britain,1992; Chapter 8. (d) Hudson, S. A.; Maitlis, P. M. *Chem. Rev.* **1993**, *93*, 861. (e) Serrano, J. L. *Metallomesogens*; Serrano, J. L., Ed.; VCH: Weinheim, Germany, 1995.

(2) (a) Barberá, J.; Espinet, P.; Lalinde, E.; Marcos, M.; Serrano, J. L. *Liq. Cryst.* **1987**, *2*, 833. (b) Espinet, P.; Etxebarría, J.; Marcos, M.; Pérez, J.; Remón, A.; Serrano, J. L. *Angew. Chem.* **1989**, *101*, 1076; *Angew. Chem., Int. Ed. Engl.* **1989**, *28*, 1065. (c) Espinet, P.; Lalinde, E. ; Marcos, M.; Pérez, J.; Serrano, J. L. *Organometallics* **1990**, *9*, 555. (d) Espinet, P.; Pérez, J.; Marcos, M.; Ros, M. B.; Serrano, J. L.; Barberá, J.; Levelut, A. M. *Organometallics* **1990**, *9*, 2028. (e) Ros, M. B.; Ruiz, N.; Serrano, J. L.; Espinet, P. *Liq. Cryst.* **1991**, *9*, 77. (f) Baena, M. J.; Espinet, P.; Ros, M. B.; Serrano, J. L. *Angew. Chem.* **1991**, *103*, 716; *Angew. Chem., Int. Ed. Engl.* **1991**, *30*, 711. (g) Baena, M. J.; Buey, J.; Espinet, P.; Kitzerow, H. S.; Heppke, G. *Angew. Chem.* **1993**, *105*, 1238; *Angew. Chem., Int. Ed. Engl.* **1993**, *32*, 1201. (h) Baena, M. J.; Espinet, P.; Ros, M. B.; Serrano, J. L.; Ezcurra, A. *Angew. Chem.* **1993**, *105*, 1260; *Angew. Chem., Int. Ed. Engl.* **1993**, *32*, 1203.

(3) See, for example: (a) Ghedini, M.; Pucci, D.; de Munno, G.; Viterbo, D.; Neve, F., Armentano, S. *Chem. Mater.* **1991**, *3*, 65. (b) Ghedini, M.; Pucci, D.; Cesarotti, E.; Francescangeli, O.; Bartolino, R. *Liq. Cryst.* **1993**, *15*, 331. (c) Ghedini, M.; Pucci, D.; Armentano, S.; Bartolino, R.; Versace, C.; Cipparrone, G.; Scaramuzza, N. N. Italian Patent VE92A000 003, 1992.

(4) Omenat, A.; Ghedini, M. *J. Chem. Soc., Chem. Commun.* **1994**, 1309.

(5) Bruce, D. W.; Liu, X. H. *J. Chem. Soc., Chem. Commun.* **1994**, 729.

(6) Pregosin, P. S.; Wombacher, F.; Albinati, A.; Lianza, F. J. *J. Organomet. Chem.* **1991**, *418*, 249.

(7) Diez, L.; Espinet, P.; Miguel, J. A. *Third International Symposium on Metallo-Mesogens*; Peñíscola, Spain, June 3−5, 1993; Abstract No. 11.

(8) Praefcke, K.; Bilgin, B.; Pickardt, J.; Borowsski, M. *Chem. Ber.* **1994**, *127*, 1543

(9) Praefcke, K.; Bilgin, B.; Usol'tseva, N.; Heinrich, B.; Guillon, D. *J. Mater. Chem.* **1995**, *5*, 2257.

(10) Mabbot, D. J.; Mann, B. E.; Maitlis, P. M. *J. Chem. Soc., Dalton Trans.* **1977**, 294.

(11) Sierra, T.; Serrano, J. L.; Ros, M. B.; Ezcurra, A.; Zubic, J. *J. Am. Chem. Soc.* **1992**, *114*, 7645.

(12) Baena, M. J.; Espinet, P.; Lequerica, M. C.; Levelut, A. M. *J. Am. Chem. Soc.* **1992**, *114*, 4182.

S0897-4756(96)00202-5 CCC: $12.00

microanalyzer. IR spectra were recorded on a Perkin-Elmer 833 spectrophotometer using Nujol mulls between polyethylene plates. ^{1}H NMR spectra were recorded on a Bruker AC-300 instrument. Microscopic studies were carried out in a Leitz microscope provided with a hot stage and polarizers. For differential scanning calorimetry a Perkin-Elmer DSC7 instrument was used, which was calibrated with water and indium; the scanning rate was 10 °C min^{-1}.

Synthesis of the Complexes. *[Pt$_2$(μ-Cl)$_2$(L$_n$)$_2$] (**2**).* To a suspension of di-μ-chlorobis(η^3-2-methylallylplatinum) (0.53 g, 0.928 mmol) in dry MeOH (35 mL) under nitrogen was added the imine **1** (1.90 mmol), and the mixture was refluxed for 24 h. After cooling, the dark green precipitate was collected on a frit, washed with MeOH (2 × 5 mL), dissolved in dichloromethane, and filtered through silica to remove the platinum metal. The resulting orange solution was concentrated, and addition of methanol gave an orange precipitate, which was filtered and vacuum dried.

2a. Yield: 55%. IR (Nujol, cm^{-1}): $\nu_{C=N}$ 1610; ν_{Pt-Cl} 333, 307. Anal. Calcd for $C_{50}H_{68}N_2Cl_2O_4Pt_2$: C, 49.14; H, 5.61; N, 2.29. Found: C, 49.01; H, 5.45; N, 2.27.

2b. Yield 72%. IR (Nujol, cm^{-1}): $\nu_{C=N}$ 1605; ν_{Pt-Cl} 318, 307. Anal. Calcd for $C_{34}H_{36}N_2Cl_2O_4Pt_2$: C, 40.93; H, 3.64; N, 2.81. Found: C, 40.93; H, 3.64; N, 2.80.

*[Pt$_2$(μ-OAc)$_2$(L$_n$)$_2$] (**3a**).* Silver acetate (0.030 g, 0.180 mmol) and **2a** (0.100 g, 0.081 mmol) in 30 mL of acetone were stirred for 2 h in the dark. The AgCl precipitate was filtered off, and the red solution was evaporated to dryness. The residue was dissolved with diethyl ether, evaporated to a small volume. Addition of methanol gave an orange precipitate, which was filtered, washed with 2 × 2 mL of methanol, and vacuum-dried. Yield 49%. IR (Nujol, cm^{-1}): $\nu_{C=N}$ 1611. Anal. Calcd for $C_{54}H_{74}N_2O_8Pt_2$: C, 51.09; H, 5.88; N, 2.20. Found: C, 50.72; H, 5.62; N, 2.00.

*[Pt$_2$(μ-(*R*)-ClPr)$_2$(L$_n$)$_2$] (**4a**).* A mixture of **2a** (0.100 g, 0.081 mmol) and potassium (*R*)-2-chloropropionate (0.026 g, 0.180 mmol) were stirred in dichloromethane/acetone (2:1, 30 mL) for 24 h. The red solution was evaporated to dryness, and the residue was crystallized in diethyl ether/methanol at −20 °C to give red crystals. Yield 86%. IR (Nujol, cm^{-1}): $\nu_{C=N}$ 1609. Anal. Calcd for $C_{56}H_{76}N_2Cl_2O_8Pt_2$: C, 49.23; H, 5.60; N, 2.05. Found: C, 49.07; H, 5.39; N, 2.05.

*[Pt$_2$(μ-SC$_6$H$_{13}$)$_2$(L$_n$)$_2$] (**5a**).* To a solution of **3a** (0.100 g, 0.079 mmol) in dichloromethane (30 mL) was added HSC_6H_{13} (22.2 μL, 0.158 mmol). The orange solution was stirred overnight, filtered through Celite, and evaporated to ca. 3 mL under reduced pressure. Addition of methanol afforded compound **5a** as a yellow-orange solid, which was filtered and washed with 2 × 3 mL of methanol. Yield 48%. IR (Nujol, cm^{-1}): $\nu_{C=N}$ 1606. Anal. Calcd for $C_{62}H_{94}N_2O_4Pt_2S_2$: C, 53.74; H, 6.84; N, 2.02. Found: C, 53.66; H, 6.70; N, 2.00.

*[Pt$_2$(μ-SC$_4$H$_9$)$_2$(L$_n$)$_2$] (**5b**).* To a suspension of **2b** (0.100 g, 0.100 mmol) in dichloromethane (30 mL) was added $AgSC_4H_9$ (0.059 g, 0.301 mmol). The mixture was stirred in the dark for 24 h. The orange solution was filtered through Celite and evaporated to ca. 3 mL under reduced pressure. Addition of methanol afforded **5b** as an orange solid, which was filtered and washed with 2 × 3 mL of methanol. Yield 76%. IR (Nujol, cm^{-1}): $\nu_{C=N}$ 1610. Anal. Calcd for $C_{42}H_{54}N_2O_4Pt_2S_2$: C, 45.64; H, 4.92; N, 2.53. Found: C, 45.44; H, 4.83; N, 2.38.

*[Pt$_2$(μ-SR)(μ-Cl)(L$_n$)$_2$] (**6**).* To a solution of **2** (0.296 mmol) in 35 mL of dichloromethane was added $AgSC_nH_{2n+1}$ (0.300 mmol). The mixture was stirred in the dark for 24 h at room temperature. After filtering off the AgCl precipitate, methanol (10 mL) was added, and the resulting solution was concentrated to a small volume. An orange solid appeared which was filtered, washed with methanol (2 × 3 mL) and air-dried. **6a**: Yield 93%. IR (Nujol, cm^{-1}): $\nu_{C=N}$ 1610. Anal. Calcd for $C_{56}H_{81}ClN_2O_4Pt_2S$: C, 51.58; H, 6.26; N, 2.16. Found: C, 51.68; H, 6.06; N, 2.15.

6b: Yield 68%. IR (Nujol, cm^{-1}): $\nu_{C=N}$ 1608; ν_{Pt-Cl} 333, 307. Anal. Calcd for $C_{50}H_{69}ClN_2O_4Pt_2S$: C, 49.23; H, 5.70; N, 2.30. Found: C, 48.63; H, 5.56; N, 2.20.

*[Pt$_2$(μ-SR)(μ-AcO)(L$_n$)$_2$] (**7a**).* Silver acetate (0.013 g, 0.076 mmol) was added to a solution of **6a** (0.100 g, 0.076 mmol) in 30 mL of acetone. The workup was as described for **6**, affording **7a** as an orange solid. Yield 52%. IR (Nujol, cm^{-1}): $\nu_{C=N}$ 1610. Anal. Calcd for $C_{58}H_{84}N_2O_6Pt_2S$: C, 52.48; H, 6.38; N, 2.11. Found: C, 52.02; H, 6.04; N, 2.19.

*[Pt$_2$(μ-SR)(μ-(*R*)-ClPr)(L$_n$)$_2$] (**8**).* A mixture of **6** (0.115 mmol) and potassium (*R*)-2-chloropropionate (0.126 mmol) in dichloromethane/acetone (2:1, 30 mL) was stirred for 24 h at room temperature. After removing the precipitate by filtration, the resulting solution was concentrated to dryness. The residue was triturated in a mixture of dichloromethane/methanol (1/3) to obtain a yellow solid, which was filtered, washed with 2 × 3 mL of methanol, and air-dried.

8a: Yield: 66%. IR (Nujol, cm^{-1}): $\nu_{C=N}$ 1607. Anal. Calcd for $C_{59}H_{85}ClN_2O_6Pt_2S$: C, 51.50; H, 6.23; N, 2.04. Found: C, 51.23; H, 6.02; N, 1.98.

8b: Yield 55%. IR (Nujol, cm^{-1}): $\nu_{C=N}$ 1608. Anal. Calcd for $C_{53}H_{73}ClN_2O_6Pt_2S$: C, 49.28; H, 5.70; N, 2.17. Found: C, 49.20; H, 5.55; N, 1.93.

*[Pt(acac)L$_n$] (**9**).* [Pt$_2$(μ-Cl)$_2$(L$_n$)$_2$] (**2**, 0.327 g, 0.267 mmol) in 35 mL of dichloromethane was reacted with a stoichiometric amount of [Tl(acac)] (0.162 g, 0.534 mmol). After 2 h stirring the white precipitate of TlCl was filtered off, the solution was evaporated to dryness, and the residue was stirred with 10 mL of methanol to give the complex as an orange solid.

9a: Yield 87%. IR (Nujol, cm^{-1}): $\nu_{C=N}$ 1606. Anal. Calcd for $C_{30}H_{41}NO_4Pt$: C, 53.40; H, 6.12; N, 2.08. Found: C, 53.47; H, 5.97; N, 2.01.

9b: Yield 80%. IR (Nujol, cm^{-1}): $\nu_{C=N}$ 1609. Anal. Calcd for $C_{22}H_{25}NO_4Pt$: C, 46.97; H, 4.48; N, 2.49. Found: C, 46.79; H, 4.39; N, 2.41.

Results and Discussion

Syntheses and Structures. The synthetic procedures leading to the different orthoplatinated complexes are illustrated in Scheme 1. The molecules have the molecular shapes sketched in Figure 1. The ^{1}H NMR spectra of the complexes are given in Table 1.

The dinuclear cycloplatinated chloro-bridged complexes **2** are prepared by reaction of the corresponding imine with [Pt$_2$(μ-Cl)$_2$(η^3-C$_4$H$_7$)$_2$] in a 2:1 molar ratio, in refluxing methanol for 24 h. Differently from its palladium analogues, where only the trans isomer is obtained,[15] the ^{1}H NMR spectrum of **2a** shows that the product is a ca. 4:1 mixture of the trans and cis isomers. Attempts at separation (by recrystallization or column chromatography) of the isomeric mixture have been unsuccessful. The isomeric ratio does not change noticeably (by ^{1}H NMR) between 250 K and 315 K. The insolubility of **2b** precluded the recording of its NMR spectrum.

Reaction of **2a** with silver acetate or potassium (*R*)-2-chloropropionate leads to exchange of the bridging chloro ligands by acetato or (*R*)-2-chloropropionato, giving **3a** and **4a**, respectively. They are more soluble than the starting complex **2a**. Their ^{1}H NMR spectra are very similar to those of their palladium analogues,[15] and prove that: (i) the compounds are dinuclear with an open-book-shaped structure;[16] and (ii) the trans isomers is the main component (97%) for **3a**, and the only isomer for **4a**, in each case giving rise to the diastereoisomers *trans*-Δ*R*,*R* and *trans*-Λ*R*,*R*.

Complex **3a** reacts with HSC_6H_{13} to give the bis(μ-alkanethiolato) complex **5a**. There are three possible sources of isomerism in orthoplatinated dimers of the type [Pt$_2$(μ-SR)$_2$(L$_n$)$_2$], namely, (i) cis or trans arrange-

(13) Taylor, E. C.; Hawks, G. H.; Mckillop, A. *J. Am. Chem. Soc.* **1968**, *90*, 2421
(14) Keller, P., Liebert, L. *Solid. State Phys., Suppl.* **1978**, *14*, 19.
(15) Buey, J.; Espinet, P. *J. Organomet. Chem.* **1996**, *507*, 137.
(16) Ciriano, M. A.; Espinet, P.; Lalinde, E.; Ros, M. B.; Serrano, J. L. *J. Mol. Struc.* **1987**, *196*, 327.

Scheme 1

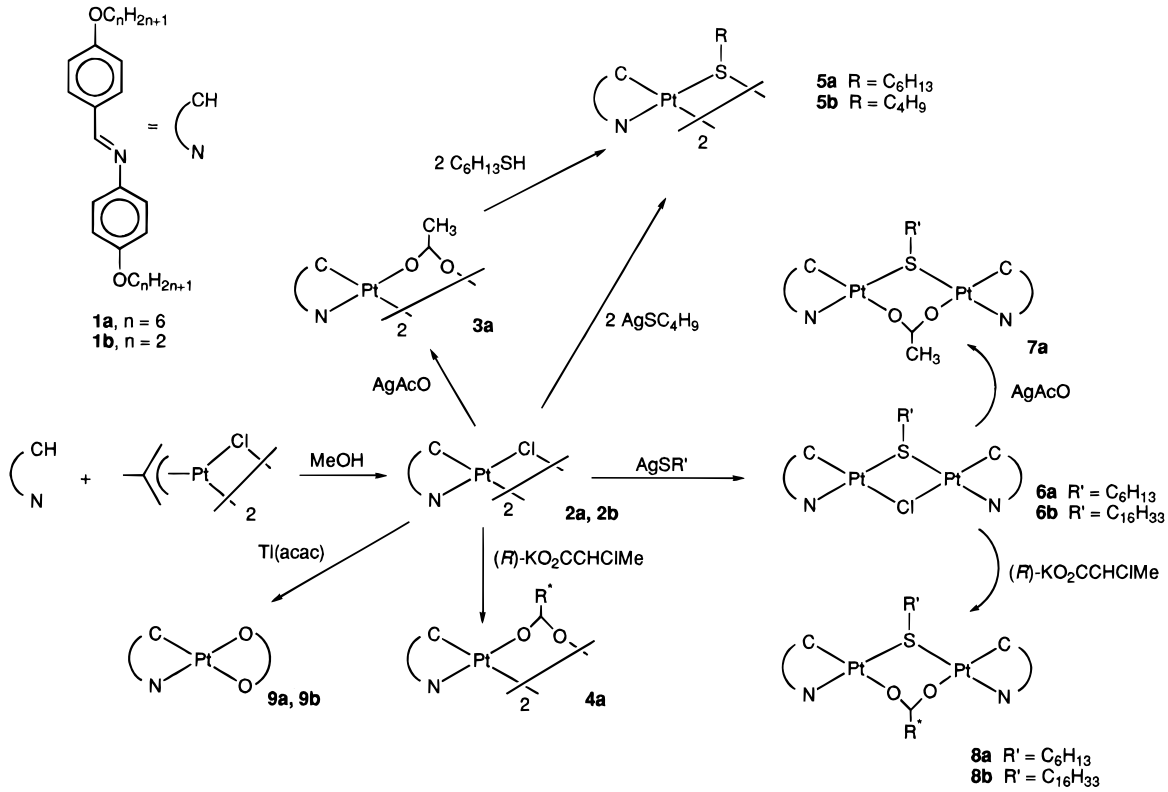

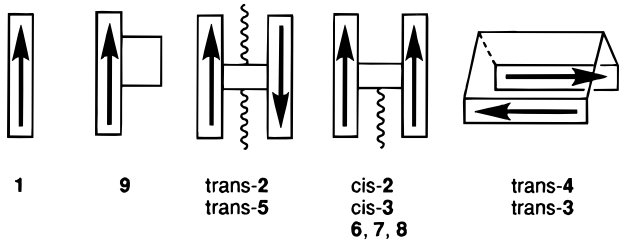

Figure 1. Schematic representation of the shapes of the molecules types in Scheme 1. The arrows indicate the relative orientation of the imine moieties. The wavy lines indicate long chains not connected to aromatic rings (none for **2** or **3**, one for **6**, **7**, or **8**; two for **5**).

ment of the two imine moieties, (ii) syn or anti configuration of the SR groups, according to whether the R groups on sulfur are on the same or on opposite sides of the Pt_2S_2 system, and (iii) flat or hinged (on the line connecting the sulfur atoms). Although isomers of the last two types have been observed,[17] fluxional processes fast on the NMR time scale explain why syn or anti and flat or hinged isomers with respect to the sulfur atoms cannot be detected here.[18] Theoretical calculations support that the energy difference between the planar and the hinged structures is rather low, making the hinging motion easy.[19] In fact the ^{1}H NMR spectrum of **5a** in $CDCl_3$ shows only a mixture of cis and trans isomers in a ratio 15:85, calculated from the intensity of two types of protons signals. As expected, the trans isomer shows only one SCH_2 signal (triplet with ^{195}Pt satellites). The cis isomer shows two sets of SR signals, some of them overlapped and submerged by the alkoxy chain of the imine. The signal of the first methylene of one thiolato group shows a normal chemical shift, 2.95 ppm, and is assigned to the chain cis to the metalated carbon atoms. The SCH_2 group of the other thiolato chain, cis to the nitrogen atoms, is located in the region of anisotropic shielding by the close phenyl groups,[20] which causes an upfield shift, and the signal is obscured by other methylenic protons of the chain. To obtain the NMR parameters of the thiolate bridging groups with cis or trans arrangement of the imines, **5b** (with short alkoxylic and thiolate chains, $n = 2$ and $n = 4$, respectively) was prepared. The use of homonuclear shift correlation spectroscopy (COXY) makes the assignment of resonances possible (Table 1). In this way the shielding effect in the signals corresponding to the SR chain cis to the iminic nitrogens (in the cis complex) was confirmed unambiguously. This observation was further used for structure assignment of other complexes.

Treatment of **2a** and **2b** with $AgSC_nH_{2n+1}$ ($n = 6$, 16; Pt/Ag = 2/1) produces the corresponding binuclear complexes **6a** and **6b**, containing mixed chlorothiolato bridges. They react with silver acetate (1:1) or potassium (*R*)-2-chloropropionate (1:1.1) yielding the mixed-bridge thiolatocarboxylato complexes **7a** or **8a**, **8b,** respectively. The ^{1}H NMR resonances of the orthoplatinated imine ligand indicate the isomeric purity of the complexes and a cis arrangement of the two imine moieties in these complexes. An arrangement with the thiolato group trans to the iminic nitrogens is proposed in agreement with the usual antisymbiotic behavior of the soft platinum atom, leading to cis arrangement of the softer ligands (carbon and sulfur).[21] This assign-

(17) Capdevila, M.; Clegg, W.; González-Duarte, P.; Harris B.; Mira, I.; Sola J.; Taylor, I. C. *J. Chem. Soc., Dalton Trans.* **1992**, 2817 and references therein.
(18) Brown, M. P.; Puddephatt, R. J.; Upton, C. E. E. *J. Chem. Soc., Dalton Trans.* **1976**, 2490.
(19) Capdevila, M.; Clegg, W.; González-Duarte, P.; Jarid, A.; Lledós, A. *Inorg. Chem.* **1996**, *35*, 490.
(20) Akitt, J. W. *NMR and Chemistry*, 2nd ed.; Chapman and Hall Ltd.: London, 1983.
(21) Hartley, F. R. *Chem. Soc. Rev.* **1973**, *2*, 163.

Table 1. ^{1}H NMR Parameters for Compounds 2−9[a]

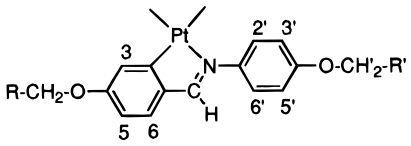

comp	H[b]	H3[b,c]	H5[d]	H6[e]	H2′6′,H3′5′[f]	OCH_2/OCH'_2[g]	others[h]
1a	8.39 s	6.94	6.94	7.81	7.18, 6.90	4.01, 3.96	
2a-*trans*	7.90 s [147]	6.73 d	6.55 dd	7.22 d	7.32, 6.90	3.97 m	
2a-*cis*[i]	7.88 s	6.92 d			7.21, 6.79	4.05 t	
3a	7.58 s [140]	6.11 d	6.56 dd	7.16 d	6.73, 6.67	3.92, 3.70 m	1.99 s CH_3CO_2
4a	7.57 s [140]	6.07 d, 6.05 d	6.57 dd	7.18 d	6.64 m	3.91, 3.71 m	4.42 q, 4.38 q (6.7) C*H*Cl; 1.57 d (6.7) CH_3CHCl
5a-*trans*	8.18 s [89]	6.97 d	6.55 dd	7.33 d	7.31, 6.93	4.00 t, 3.99 t	2.14 m SCH_2
5a-*cis*	8.08 s [89]	7.35 d	6.57 dd	7.33 d	7.28, 6.82	4.08 t, 3.93 t	2.94 m SCH_2
5b-*trans*	8.18 s	6.96 d			6.93		2.15 m SCH_2; 1.80 m SCH$_2$-CH_2; 1.10 m SCH$_2$-CH$_2$-CH_2; 0.70 t CH_3
5b-*cis*	8.09 s [91]	7.34 d [53]	6.57 dd	7.33 d	7.26, 6.82	4.16 q, 4.01 q	2.90[j] m SCH_2; 2.20 m SCH$_2$-CH_2; 1.55 m SCH$_2$-CH$_2$-CH_2; 0.97 t CH_3 0.75[k] m SCH_2; 1.30 m SCH$_2$-CH_2; 0.58 m SCH$_2$-CH$_2$-CH_2; 0.50 t CH_3
6a	8.08 s [93]	7.33 d	6.57 dd	7.28 d	7.22, 6.82	4.06 m	2.95 m SCH_2
6b	8.08 s [102]	7.33 d	6.57 dd	7.28 d	7.21, 6.81	4.14 m, 4.02 q	2.94 m SCH_2
7a	8.12 s [105]	7.59 d	6.50 dd	7.23 d	7.29, 6.86	4.08 m	2.46 m SCH_2; 1.66 s CH_3CO_2
8a	8.03 s, 8.02 s [102]	7.59, 7.57 [60]	6.50 d	7.21 d	7.21 m, 6.84 m	4.09 m, 3.86 m	3.95 m C*H*Cl; 2.48 m SCH_2; 1.01 d (6.7) CH_2CHCl
8b	8.03 s [103]	7.60 d, 7.59 d [63]	6.50 dd	7.21 d	7.20 m, 6.83 m	4.15 m, 3.95 m	3.99 m C*H*Cl; 2.48 m SCH_2; 1.01 d (6.7) CH_2CHCl
9a	8.12 s [128]	7.11 d [43]	6.60 dd	7.33 d	7.37, 6.89	4.08 t, 3.98 t	5.41 s C*H*; 1.98 s, 1.79 s CH_3CO
9b	8.11 s [128]	7.12 d [42]	6.59 dd	7.33 d	7.36, 6.88	4.16 q, 4.05 q	5.40 s C*H*; 1.97 s, 1.78 s CH_3CO

[a] In $CDCl_3$ at 300.13 MHz; the numbers in parentheses correspond to $J(^1H-^1H)$ in hertz; the numbers in square bracket correspond to $^3J(^{195}Pt-^1H)$ in Hz, s, singlet; d, doublet; t, triplet; q, quartet; m, multiplet. [b] Some satellites due to ^{195}Pt coupling were not identified due to their low intensities or broadness. [c] $J_{H3-H5} = 2.3$ Hz. [d] $J_{H5-H6} = 8.3$ Hz, $J_{H5-H3} = 2.3$ Hz. [e] $J_{H6-H5} = 8.3$ Hz. [f] $(AB)_2$ spin system with $J_{HA-HB} = 8.9$ Hz. [g] $^3J_{H-H} = 6.6$ Hz. [h] Aliphatic protons (R and R′) of compounds **2a**, **3a**, **4a**, **5a**, **6a**, **7a**, **8a**, **9a** appear in the range $\delta = 0.8-1.9$ ppm. Compound **8b** CH_3 δ 1.45 t, CH'_3 δ 1.37 t, compound **9b** CH_3 δ 1.44 t, CH'_3 δ 1.43 t. [i] Cis or trans signals overlapped by trans or cis signals. [j] Aliphatic protons of the thiolato group trans to the iminic nitrogens. [k] Aliphatic protons of the thiolato group cis to the iminic nitrogens.

ment is supported by the chemical shift of the SCH_2 protons, and the X-ray diffraction structure determined for the palladium analogue [Pd_2(*p*-$C_4H_9O-C_6H_3-CH{=}NC_6H_4OC_4H_9$-*p*)$_2$(*μ*-Cl)(*μ*-SR)] shows the arrangement proposed.[22] A somewhat folded structure is expected for the types of complexes **7** and **8.** The isomer proposed is that reported for [Pd_2($CH_2C_9H_6N$)$_2$(*μ*-O_2CCF_3)(*μ*-SBu^t)] ($CH_2C_9H_6N$ = 8-quinolylmethyl).[23] In solution at room temperature, a fast dynamic process averages the molecule to planar on the NMR time scale.

Finally, the mononuclear species **9a** and **9b** are obtained by reaction of the binuclear complexes **2a** and **2b** with [Tl(acac)].

Comparison of the ^{1}H NMR parameters of these platinum complexes with those of their palladium analogues shows that the main difference is the chemical shifts observed for the iminic proton and for H^3, while the rest of the signals are not, or just slightly modified.

Other significant feature of ^{1}H NMR spectra of the platinum complexes is the $^3J_{Pt-H}$ values for the iminic protons. Some of them are very large compared with previous values reported for other orthoplatinated imines.[6,24−27] It seems that the range of $^3J_{Pt-H}$ values depends strongly on the ligand trans to the iminic nitrogen. The variation observed is as follows (trans ligand, and range of $^3J_{Pt-H}$ values in parentheses): Me^- (50−62 Hz)[24−27] > SR^- (89−105 Hz) ≈ PPh_3 (97 Hz)[6] > $acac^-$ (128 Hz) > OAc^- (140 Hz) ≈ $Cl^-_{bridging}$ (147 Hz). The order of increasing $^3J_{Pt-H}$ is consistent with the order of decreasing trans influence.[28]

Mesogenic Behavior. Table 2 summarizes the transition temperatures, enthalpies, and types of mesophase observed for the platinum complexes. All the platinum compounds synthesized show mesogenic properties except the nonplanar acetato complex **3a**. In general the dinuclear compounds display a smectic A phase showing the typical mielinic and homeotropic textures, reorganizing to the fan-shaped texture at temperatures close to the clearing point, and the focal-conic fan texture on cooling from the isotropic liquid. The exception is **8b**, which shows a cholesteric phase. As observed also for the Pd analogue,[15] **4a** shows a double melting behavior, a kinetic effect extensively studied by Otha et al.[29] The transitions to the isotropic liquid occur with extensive decomposition for the complexes with clearing points above 200 °C.

(22) Buey, J.; Díez, G. A.; Espinet, P.; García-Granda, S.; Pérez-Carreño, E., to be published.
(23) Ruiz, J.; Cutillas, N.; Torregrosa, J.; García G.; López, G.; Chaloner, P. A.; Hitchcock, P. B.; Harrison, R. M. *J. Chem. Soc., Dalton Trans.* **1994**, 2353.
(24) Anderson, C. M.; Crespo, M.; Jennings, M. C.; Lough, A. J.; Ferguson, G.; Puddephatt, R. J. *Organometallics* **1991**, *10*, 2672.
(25) Crespo, M.; Martínez, M.; Sales, J.; Solans, X.; Font-Bardía, M. *Organometallics* **1992**, *11*, 1288.
(26) Crespo, M.; Martínez, M.; Sales, J. *Organometallics* **1993**, *12*, 4297.
(27) Crespo, M.; Solans, X.; Font-Bardía, M. *Organometallics* **1995**, *14*, 355.
(28) Appleton, T. G.; Clark, H. C.; Manzer, L. E. *Coord. Chem. Rev*, **1973**, *10*, 335.
(29) (a) Otha, K.; Yokohama, S.; Kusabayashi, S.; Mikawa, H. *J. Chem. Soc., Chem. Commun.* **1980**, 392. (b) Ohta, K.; Muroki, H.; Hatada, K. I.; Yamamoto, I.; Matsuzaki, K. *Mol. Cryst. Liq. Cryst.* **1985**, *130*, 249. (c) Ohta, K.; Muroki, H.; Hatada, K. I.; Takagi, A.; Ema, H.; Yamamoto, I.; Matsuzaki, K. *Ibid.* **1986**, *140*, 163. (d) Ohta, K.; Muroki, H.; Ema, H.; Yamamoto, I.; Matsuzaki, K. *Ibid.* **1987**, *147*, 61.

Table 2. Optical, Thermal, and Thermodynamic Data for Compounds 2−9[a]

comp	transition	T/°C	ΔH/kJ mol^{-1}
2a	C−S_A	163.8	22.3
	S_A−I	260.0[b]	
2b	C−S_A	256.0	45.0
	S_A−I	268.0[b]	
3a	C−I	201.9[b]	70.4
4a	C−S_A	141.7	16.0
	S_A−I	187[c]	
	I−$S_{A'}$	188[c]	
	$S_{A'}$−I	200[b,c]	
5a	C−S_A	149.5	61.1
	S_A−I	162.4	10.5
5b	C−C′	197.4	1.5
	C′−I	220.2	75.9
	I−N	146.0[d,e]	−1.2
6a	C−S_A	160.4	27.4
	S_A−I	241.7	7.1
7a	C−C′	134.8	3.0
	C′−S_A	179.8	22.3
	S_A−I	206.6	5.1
8a	C−C′	51.4	3.7
	C′−S_A	112.0	25.6
	S_A−I	185.0	1.4
8b	C−Ch	119.7	26.9
	Ch−I	132.9	0.3
9a	C−S_A	110.7	35.9
	S_A−N	136.4	0.7
	N−I	142.5	1.1
9b	C−I	213.0	40.2
	I−N	145.5[d]	−1.2
	N−C	116.7[d]	−16.5

[a] C = crystal; S_A smectic A; Ch = cholesteric; N = nematic; I = isotropic liquid. [b] Decomposition. [c] Observed by means of polarized light microscopy only. [d] Monotropic transition. [e] A glassy mesophase is obtained on cooling but the T_g cannot be appreciated in the DSC.

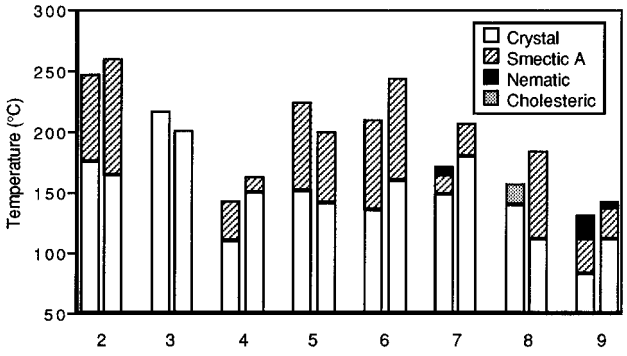

Figure 2. Thermotropic behavior of similar Pd and Pt materials (hexyloxy derivatives; on each pair the left bar is the Pd compound). The number in the abscisa indicates the molecular type, as labeled in Scheme 1.

The change in molecular shape from the dinuclear complexes to the mononuclear acetylacetonate derivatives **9** ("P-shaped" geometry) produces, as expected from our previous observations in palladium,[2f,15] a noticeable lowering of both the melting and the clearing temperatures. In addition to a smectic A phase **9a** exhibits a nematic phase and can be taken repeatedly into the isotropic state without showing signs of decomposition.

Figure 2 plots the mesogenic properties of the platinum hexyloxy complexes versus those of their palladium analogues. The behavior of the transition temperatures on going from Pd to Pt is not regular, but it must be considered that some Pt compounds (**2a**, **3a**, **4a**, and **5a**) have an isomeric composition different from that of their Pd analogues. For this reason, the significance of their transition temperatures is probably low.

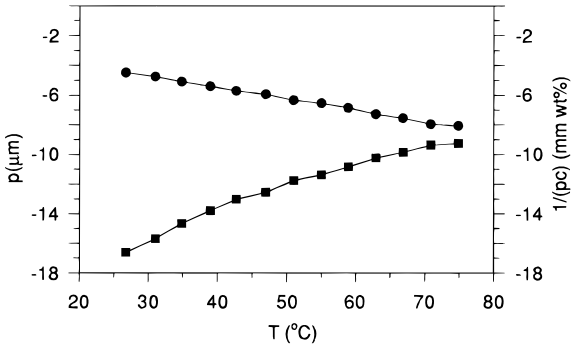

Figure 3. Temperature dependence of the cholesteric helical pitch (p) (■) and the helical twisting power ($1/pc$; (●) c = concentration of the chiral compound in wt %) for a mixture of **8b** (13.44 wt%) and the commercial nematic solvent ZLI-1275.

In **6**, **7**, **8**, and **9** the Pd and Pt complexes are isomerically pure and present the same structure. In these complexes the clearing temperatures are consistently higher for the Pt derivatives. Thus, the effect of replacing Pd by the heavier Pt (with the consequent enhancement in polarizability) is to increase noticeably the transition temperatures. This is in contrast with the observations made on disk-shaped tetra-Pd and tetra-Pt organyl complexes, where the change in metal scarcely influences the thermal properties.[9] Thus, tuning of the properties of a metallomesogen by exchange of isostructural metals can be achieved better in calamitic than in discotic molecules, as in the latter the metal is very hidden in the molecule.[9]

The mesogenic properties of **8a** were disappointing compared to those of its Pd analogue.[15] The Pd complex is cholesteric whereas the Pt complex is smectic A. By decreasing the chain length of the imine (to $n = 2$) and increasing the thiolato chain (to $n = 16$) a material was obtained, **8b**, displaying an enantiotropic cholesteric mesophase, while for the Pd analogue only a monotropic phase had been observed. The pitch (p) and helical twisting power ($1/pc$) induced by **8b** in mixtures of the Pt complex (13.44% in weight) and ZLI-1275 (a commercial nematic solvent supplied by Merck, 1,4-didodecanoxyhydroquinone) were measured by applying the Grandjean−Cano method,[30] and the results are shown in Figure 3. **8b** shows a left-handed helix ($p < 0$) in the range investigated, and a temperature dependence which suggests that an inversion of the helical screw sense might occur at lower temperatures. This phenomenon has been observed in Pd mesogens,[2g] but the p and $1/pc$ variation with temperature in Pt is slower.

The cholesteric phase of **8b** gets frozen in a glasslike state on cooling, which makes the material adequate for optical storage as described below.

Optical Storage Effect. Compound **8b** shows absorption in the visible wavelength range and exhibits a glasslike liquid-crystalline state at room temperature. Thus, it is possible to vary its optical properties due to opto-optical or thermo-optical effects. Light-induced structures can be stored in the glasslike state. Similar storage effects have been demonstrated for liquid-crystal polymers,[31,32] for polymer-dispersed liquid crystals,[33,34]

(30) Heppke, H.; Oestreicher, F. *Mol. Cryst. Liq. Cryst. Lett.* **1978**, *41*, 245.
(31) Eich, M.; Wendorff, J. H. *Makromol. Chem., Rapid Commun.* **1987**, *8*, 59.
(32) Anderle, K.; Wendorff, J. H. *Mol. Cryst. Liq. Cryst.* **1994**, *243*, 51.

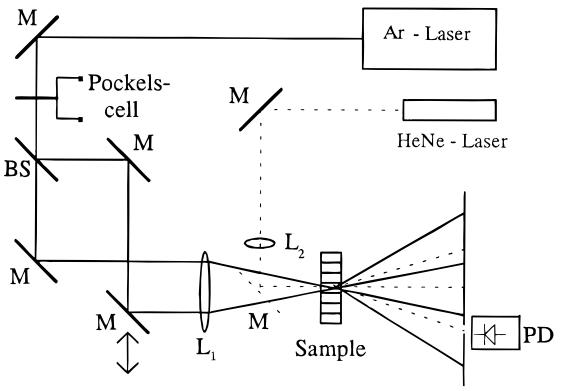

Figure 4. Experimental setup used for the grating formation by interference of two laser beams. M, mirrors; BS, beam splitter; L, lenses; PD, photo diode.

and recently for low molar mass liquid crystals which exhibit a glass-like state.[35,36] In the latter case, the liquid crystals were doped with a dichroic dye in order to promote the thermo-optical effect. This is the first time that such an effect is produced using a metallomesogen. The organometallic compound **8b** has the advantage that it shows absorption of visible light, so that opto-optical effects occur even in the pure compound. The addition of a dye is unnecessary.

To demonstrate the storage capability of **8b**, we used a holographic technique (Figure 4). A light intensity grating was generated in the sample by the interference of two coherent Ar-ion laser beams which are focused on the same spot of the sample. The difference between the angles of light incidence of the two laser beams was $\Delta\Theta = 3.32°$ which results in a lattice constant of $\Lambda = \lambda/\{2 \sin(\Delta\Theta/2)\} \approx 9\ \mu$m. The transverse intensity distribution of the single laser beams is a Gaussian with a diameter $d \approx 100\ \mu$m (full width at half of the maximum intensity). The laser power was varied up to $P = 120$ mW/beam, corresponding to a total laser intensity of $I = 2P/(\pi d^2) \approx 760$ W/cm^2. Glass cells from EHC (Japan) with a cell gap of 4 μm were used. Their surfaces are coated with polyimide and rubbed in order to promote a uniform parallel alignment of the director at the glass/liquid crystal interface. The cells were filled with the liquid crystal at elevated temperature, and the liquid crystal was allowed to align uniformly in the Grandjean texture before cooling the sample to the glass state. The measurements were performed at 22 °C, i.e., below the glass transition temperature T_g.

Exposure of these samples to the intensity grating produced by the two interfering laser beams lead to a gratinglike variation of the optical properties of the sample (Figure 5). We attribute the formation of these grating structures to the gratinglike spatial variation of the temperature within the sample. The temperature grating causes a local heating of the sample above the glass transition temperature at the positions with maximum intensity. At these positions, the refractive index can change due to the density change and due to reorientation of the director. The sample returns completely to the glasslike state as soon as the exposure to the laser beams is interrupted. Thus, the light-induced gratings are stored after the exposure. Erasure of the stored structure is possible by heating the whole sample above the glass transition temperature.

To characterize the efficiency of the stored gratings, we investigated the diffraction pattern of a 2 mW HeNe laser ($\lambda = 633$ nm) due to the grating structures induced in the sample. If $\mathbf{k}$ is the wave vector of the incident HeNe beam, the wave vector of the diffracted beam of the order m is given by $\mathbf{k}_m = \mathbf{k} + m\mathbf{Q}$, where $m = 0, \pm1, \pm2, \ldots$. The extent of the grating formation is usually characterized by the grating efficiency $\eta = I_1/I_\Sigma$, where I_Σ and I_1 are the intensities of the incident beam and the first order diffraction spot ($m = \pm1$), respectively. For a homogeneous sample with small variations of the complex refractive index, the diffraction efficiency η is given by $\eta = (\pi\delta n d/\lambda)^2 + (\Delta K d/4)^2$, where δn and ΔK are the amplitudes of the variation of the refractive index and the absorption coefficient, respectively.[37]

Figure 6 shows the diffraction efficiency and the time constant of the grating formation as a function of the power of the Ar ion laser beams. The efficiency η increases with increasing laser power and reaches saturation at $P \approx 70$ mW/beam. The maximum value $\eta_{max} \approx 1\%$ corresponds to a spatial variation of the refractive index of $\delta n = 0.02$, i.e., about one-tenth of the birefringence of the liquid crystal. When the temperature of the sample during the grating formation is increased, the diffraction efficiency η_{max} increases to more than 4% and the time constants of the grating formation decrease.

The diffraction efficiency of a few per cent is typical for thin holograms where the sample thickness ($d = 4\ \mu$m in our case) is small compared to the period of the induced grating ($\Lambda = 9\ \mu$m), so that many diffraction spots of higher order occur. The values which we obtained for η_{max} are comparable to the diffraction efficiency which was obtained earlier for the glasslike low molar mass liquid crystals using a similar geometry,[35,36] and with the diffraction efficiency which was reported for thin holograms in liquid crystalline polymers.[31] However, it is well known that volume holograms (with $\Lambda << d$) show only one diffraction spot of the first order and can thus show a diffraction efficiency up to 100%.[37] Indeed values of $\eta_{max} \approx 50\%$ have been reported for volume holograms in liquid-crystalline polymers.[32] Thus, we expect that the maximum diffraction efficiency can be enhanced by increasing the angle between the interfering beams thereby reducing the grating period.

The dynamics of the grating formation is characterized by a two-step mechanism with two different time constants. When the exposure of the sample to the Ar-laser beams is started, we observe an increase of the diffraction efficiency with a time constant τ_1 of a few seconds. Subsequently, the efficiency continues to increase slowly. To characterize this second process, we define τ_2 as the exposure time which is required to achieve 90% of the maximum diffraction efficiency. This time constant decreases with increasing laser power (Figure 6), reaching a minimum value of $\tau_2 \approx 50$ s. The more detailed investigation of the two processes of the grating formation is subject to further studies.

(33) Lackner, A. M.; Margerum, J. D.; Ramos, E.; Lim, K.-C. *Proc. SPIE* **1981**, *1080*, 53.
(34) Kitzerow, H.-S.; Strauss, J.; Jain, S. C. *Proc. SPIE* **1996**, *2651*, 80−91.
(35) Eichler, H. J.; Heppke, G.; Macdonald, R.; Schmid, H. *Mol. Cryst. Liq. Cryst.* **1992**, *223*, 159.
(36) Contzen, J.; Heppke, G.; Kitzerow, H.-S.; Krüerke, D.; Schmid, H. *Appl. Phys. B*, in press.
(37) Eichler, H. J.; Günter, P.; Pohl, D. W. *Laser-induced dynamic gratings;* Springer Series in Optical Sciences Vol. 50; Springer-Verlag: Berlin, 1986.

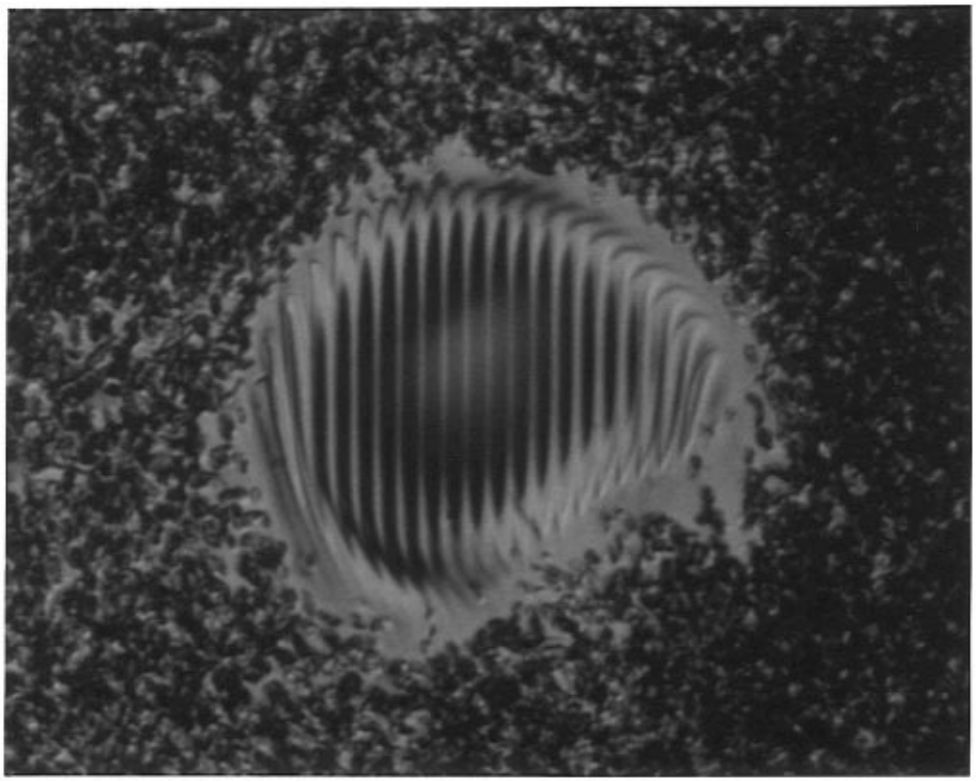

Figure 5. Photograph of the stored grating structure in compound **8b**, observed in a polarizing microscope with crossed polarizers.

Taking into account the writing intensity, the large time constants for the grating formation require a writing energy in the range of kJ/cm^2. This very high value is in the range of the writing energy reported for polymer-dispersed liquid crystals,[34] but it is much larger than the typical writing energies of less than 1 J/cm^2 which were found for other glasslike liquid crystals.[35,36] We attribute this discrepancy to the fact that our experiments were performed at room temperature and that the wavelength of $\lambda = 514$ nm does not coincide with the absorption maximum of the liquid crystal. We expect that the writing energy can be diminished by performing the experiment at a temperature close below the glass transition and by adjusting λ to the absorption band of the liquid crystal.

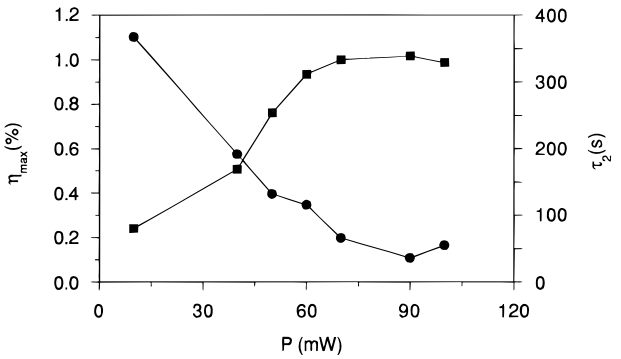

Figure 6. Diffraction efficiency η_{max} (■) and time constant for the grating formation τ_2 (●) versus power of the two laser beams which are used to generate the grating structure.

Conclusions

Calamitic orthometalated complexes of Pt can be easily made and display, in general, more ordered mesophases (some S_A in place of nematic or cholesteric) and higher transition temperatures than their Pd analogues. This reflects a higher polarizability for Pt compared to Pd.

The cholesteric compound **8b** proved to be suitable for the holographic storage of information on a glasslike cholesteric state. Grating structures with a diffraction efficiency of several percent were generated and permanently stored in the liquid-crystalline glass state. Erasure of the stored structure is possible by heating the hole sample above the glass transition temperature.

The advantage of **8b** with respect to other low molar mass liquid crystals which were previously used as storage materials is the absorption of visible light by **8b**. As a consequence, no dye has to be added in order to achieve an opto-optical effect.

Acknowledgment. We gratefully acknowledge financial support by the Spanish Comisión Interministerial de Ciencia y Tecnología (Project MAT93-0329) and the Deutsche Forschungsgemeinschaft (Sfb 335). The bilateral collaboration was supported by the Dirección General de Investigación Científica y Técnica and the Deutscher Akademischer Austauschdienst (Acciones Integradas Hispano-Alemanas No. 49B, 1995). L.D. thanks the Spanish Ministerio de Educación y Ciencia for a studentship.

CM960202N